*Desalination and Water Treatment*
www.deswater.com

doi: 10.5004/dwt.2018.22759

127 (2018) 262–271
September

# Performance analysis of biomass-based absorber solar still through ANN and MLR approach

Mande Amol Balu, D.V. Siva Krishna Rao K, M. Premalatha*

*Solar Energy Laboratory, Department of Energy & Environment (DEE), National Institute of Technology (NIT), Tiruchirappalli 620 015, Tamil Nadu, India, Tel. 04312503132; Fax: 04312500133; emails: latha@nitt.edu (M. Premalatha), amol.mande17@gmail.com (M.A. Balu), siva.damodhark@gmail.com (D.V. Siva Krishna Rao K)*

Received 20 January 2018; Accepted 9 July 2018

**ABSTRACT**

Single slope basin still having a basin area of 0.5 m$^2$ was designed and fabricated. The aim of this work was to predict the solar still productivity, using environmental and operational parameters with artificial neural network and multiple linear regressions. Individual effect of eight variables, namely global horizontal solar radiation, ambient temperature, wind speed (WS), relative humidity (RH), basin temperature, time of still operation, inner and outer glass temperatures ($T_{inner}$ and $T_{outer}$) on the estimation of still productivity were studied through linear regression. Statistical tools such as relative root mean square error, coefficient of determination ($R^2$), model efficiency and the overall index of model performance were used as performance indices to identify the best model. It is observed that $T_{inner}$ and $T_{outer}$ have the highest impact, whereas WS and RH have the least impact in predicting the still productivity.

*Keywords:* Artificial neural network; Biomass absorber; Multiple linear regressions; Solar desalination; Solar still

## 1. Introduction

The shortage of drinking water is one of the biggest problem many countries facing along with the energy shortage. With increase in population and industrial revolution demand for freshwater has been increased many folds. However, most of the available water is not suitable for direct consumption. This unsuitable water must be purified before it can be supplied to the community for consumption. Distillation is a process through which it can be achieved. The energy required for distillation is most of the times obtained from fossil fuels which has larger carbon footprint. In India, 1 kWh of electrical energy obtained from coal-based power plant is equivalent to an emission of 1 kg of $CO_2$ at the source [1] and it reaches to 1.58 kg of $CO_2$ [2–4] if losses of distribution and end appliance are included. In India more than 90% of the places have annual average global horizontal radiation (GHI) in the range of 4.5–6.0 kWh/m$^2$ d [5]. Solar still can be used at such places where sunlight and brackish water is available. Basin type solar still is simple in design and operation and can be fabricated using local materials. The main disadvantage of basin type solar still is its low productivity. The productivity of still can be improved by changing its design, operational and environmental parameters. Environmental parameters such as solar radiation intensity, wind velocity, relative humidity (RH) are site dependant and hence can't be changed. Operational parameters like feed water depth in the basin, feed water salinity, condensing cover cooling, feed water temperature and still operating under vacuum are important parameters in the improvement of productivity of solar still. Phadatare and Verma [6] concluded that with increase in depth of water in the basin, still productivity decreases. Suneesh et al. [7] used condensing cover cooling technique using cotton gauze to improve the productivity to 4.30 L/m$^2$ d, whereas without cooling it was 3.30 L/m$^2$ d. Taamneh and Taamneh [8] improved productivity by 25% using forced convection with help of fan inside the still over natural convection. The productivity of still depends upon design parameters such as type of still,

* Corresponding author.

material used for fabrication, size and shape of still, external condenser, use of reflectors, sensible and latent heat storage materials, inclination of cover, material and thickness of cover and absorber material used in the basin. Sellami et al. [9] used Portland cement, Srivastava and Agrawal [10] used expanded polystyrene to float the porous absorber and Abdallah et al. [11] used metallic wiry sponges as basin absorber material. Use of environment-friendly and porous absorber material will increase the productivity with lesser carbon footprint. To improve the overnight productivity sensible heat storage [9,12–14] and latent heat storage [15,16] was used. Various design modifications like hemispherical still [17], conical still [18], triangular pyramid still [19] and pyramid still with concave wick [20] were used to improve the productivity. Other modifications such as floating porous absorber [10] and internal reflector [21] were investigated. The disadvantage of experimental work and thermal analysis of solar distillation system is it consumes more resources and time. Also, large number of measurements and heat transfer processes are required. The available heat and mass transfer models are complex and require lengthy calculations for the results. The available models require appropriate changes so that they can be applied for modified designs. Alternatively, an artificial neural network (ANN) could be used easily to precisely forecast solar still productivity.

Mashaly et al. [22] developed a mathematical model to forecast the solar still performance under hyper-arid conditions using ANN technique. Ten parameters were considered as inputs and water productivity, operational recovery ratio and thermal efficiency were considered as outputs to ANN. A multilayer perception (MLP) type feed-forward back-propagation neural network with three layers (one input layer, one hidden layer and an output layer) was developed. The number of neurons in the hidden layer was determined through the trial and error method by varying the number of hidden nodes from 2 to 20, and the best architecture was selected with 15 neurons. They concluded that the model was effective and accurate in predicting solar still performance with insignificant errors and reported an overall index of model performance (OI) value of 0.986. Mashaly et al. [23] modelled the instantaneous thermal efficiency of a solar still, using nine variables from weather and operational data with MLP neural network and multiple linear regressions (MLRs). 160 data points obtained from the experimental study were used in the model development and validation. They concluded that the MLP model was a highly precise model in predicting the thermal efficiency compared with the MLR model. Hamdan et al. [24] developed three ANN models using feed-forward, Elman and nonlinear autoregressive exogenous networks (NARX) to find the performance of triple solar still operating under Jordanian climate with nine input variables. Total 46 samples were used with tangent sigmoid function for the hidden layer and linear transfer function for the output layer. They concluded that feed-forward model was the best model in the estimation of thermal efficiency of a triple basin solar still compared with NARX and Elman networks. Santos et al. [25] developed a model to predict the solar still distillate production from two different commercial solar stills to determine the effectiveness of modelling solar still distillate production using ANN and local weather data. Daily total insolation, daily average wind velocity, daily average cloud cover, daily average wind direction and daily average ambient temperature were considered as input variables to the ANN. Mashaly et al. [26] developed ANN models to forecast the productivity of a solar still operating in a hyper-arid environment with three different learning algorithms, namely Levenberg–Marquardt (LM), the conjugate gradient back propagation with Fletcher–Reeves restarts and the resilient back propagation. In the model development and validation 160 data points were used. Nine variables were utilized as input parameters and productivity capacity was the output of ANN. They reported that the LM learning algorithm was given an OI as 0.981 in predicting solar still productivity. They concluded that LM algorithm was given the best forecasted values among the selected algorithms.

The above studies revealed that modelling of solar still is needed to assess the performance. These models should be accurate and should use most relevant parameters as inputs to the models. In this study ANN models and MLR models are developed to estimate the solar still output by using environmental and operational parameters of the still as inputs.

## 2. Materials and methods

### 2.1. Experimental setup

The experiments were conducted at the Solar Energy Lab, Department of Energy and Environment (DEE), NIT Trichy, Trichy (10.7589°N, 78.8132°E) during the months of March and April 2016 between 8.00 and 18.00 h. The basin type solar still used in the experiments consists of two parts: (1) basin tray and (2) cover. The basin tray was fabricated using stainless steel of 1 mm thick sheet having approximately 0.5 $m^2$ (0.9 m × 0.58 m × 0.05 m) basin area. The cover was fabricated using 4 mm window glass and had double wall arrangement at the walls except at front wall with 30 mm air gap between the two walls. The cover had an inclination of 14° with the horizontal obtained with the walls having height of 260 and 40 mm at higher and lower side, respectively. To absorb the early and late hour's solar radiation, the inner side of the inner glass wall was painted with black paint whereas the outer wall was kept transparent. The basin material used was the mixture of coco peat and charcoal having 20 mm thickness. Mixture of coco peat and charcoal is organic, environment-friendly, biodegradable and easily available locally. Insulation of 20 mm thick expanded polystyrene was provided at the tray side walls and bottom. The silicone gel was used to stick the glasses, whereas glass putty was used in between the tray and cover to arrest leak of water vapour to the surrounding.

The solar still was kept on a table with its condensing cover facing due south as shown in Fig. 1. Fig. 2 shows the schematic diagram of the solar still. The feed water was supplied to the basin before the starting of the experiment every morning. Basin material was coco peat and charcoal mixture which is environment-friendly and locally available at lower cost. Coco peat being porous in nature has more surface area which results in greater evaporation of feed water. As the solar energy heats up the basin material which absorbed the water, the mixture of hot air and water vapour rises to the top of the condensing cover and then

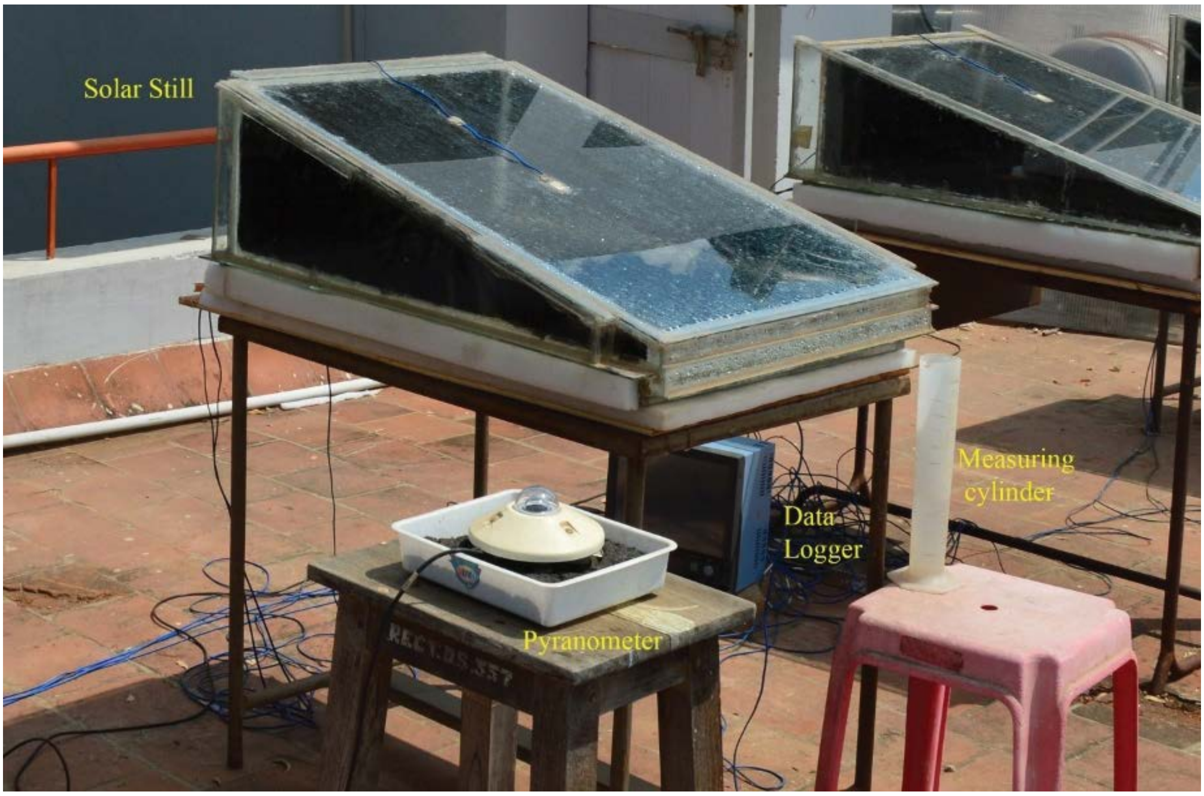


Fig. 1. Experimental setup.

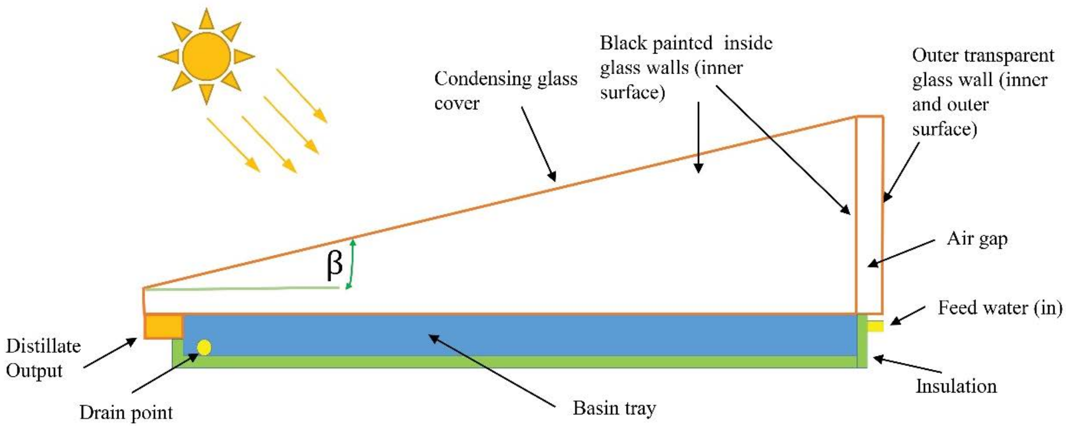


Fig. 2. Schematic diagram of solar still.

reversed the direction to reach the basin material. During this natural circulation process, the humid air comes in contact with the bottom part of the condensing cover where it releases the latent heat and gets condensed. The condensed water flows down and collected in the trough made to collect distillate. Tap water was used as a feed water to the solar still. The initial concentration of total dissolved solids (TDS), pH and electrical conductivity (EC) of the tap water were 469 mg/L, 8.96 and 781 µS/cm, respectively. TDS and EC were measured using (Hach sension5) calibrated TDS-EC meter. A pH meter (DURALAB) was used to measure pH. The basin temperature, inner and outer glass temperature were measured using thermocouples (T-type). Solar radiation intensity was measured using (Kipp & Zonen, CM11) pyranometer. Temperatures and solar radiation intensity data were recorded on data logger (Yokogava, GX20) for every 10 s. The distilled water was measured by graduated cylinder (TARSONS) of 500 mL capacity. The weather data such as ambient temperature ($T_{amb}$), RH and wind speed (WS) were obtained from a weather station near the experimental site.

The expected productivity of solar still was modelled using environmental (four variables) and operational data (four variables) with MLR and ANN. The variables affect the solar still productivity were considered as model parameters. Weather variables, namely global horizontal solar radiation ($H$), ambient temperature ($T_{amb}$), WS, RH and operational variable, namely basin temperature ($T_{basin}$), inner glass temperature ($T_{inner}$), outer glass temperature ($T_{outer}$) and time of still operation ($t$) were used in modelling the expected productivity of solar still.

### 2.2. Regression methods

Regression is one of the most widely used statistical technique for forecasting problems. Linear regression and MLR techniques were used in the present study. Regression analysis is a modelling technique for analysing the relationship between a continuous dependent variable $y$ and one or more independent variables $x_1$, $x_2$, $x_k$. The goal in regression analysis is to identify a function that describes, as closely as possible, the relationship between these variables so that the value of the dependent variables can be predicted using a range of independent variables values

In the MLR method, the output of solar still is found in terms of independent variable such as weather and other solar still variables which influence the output. This model is named as yield model. The yield model using this method is expressed in the form of Eq. (1) as follows:

$$Y = \beta_i + \beta_i x_1 + \beta_i x_2 + \cdots\cdots + \beta_i x_k + \varepsilon \quad (1)$$

where $Y$ is the yield of the solar still, $x_i$ is the affecting factors, $\beta_i$ is regression parameters with respect to $x_i$ and $\varepsilon$ is an error term. A goodness of fit measurement is represented by the coefficient of correlation ($R^2$) statistic which ranges from 0 to 1 and indicates the proportion of the total variation in the dependent variable $Y$ around its average that is counted by the independent variable in the estimated regression function. The closer the $R^2$ statistic to the value 1, the better the estimated regression function fits the data.

### 2.3. ANN model

ANN is an artificial intelligence (AI) technique that follows the behaviour of the human brain. ANN techniques have become an alternative method to the conventional techniques and are used in a number of solar energy applications. ANN has the ability to model any linear and nonlinear systems. The ANN architecture usually consists of an input layer, some hidden layers and an output layer, connection weights and biases, activation function and summation node. Functional diagram of neural network is given in Fig. 3.

ANN action is divided into two stages: learning stage and generalization stage. The learning techniques are divided as supervised, unsupervised, reinforcement and evolutionary learning. Neural networks training is such that a particular input leads to a specific target output. The network is adjusted, based on the comparison between the output and the target, until the network output matches the target and the mean square error (MSE) is determined. MSE determines the performance of the network. It measures the network's performance according to the mean of the squared errors. Learning process is completed when the MSE is minimized.

### 2.4. Test conditions

In this study, the feed forward architecture was used with the three layers (input, hidden and output layers). TRAINLM is used as training function that updates the weight and bias values of neuron connections, according to LM optimization. The back propagation algorithm is used as learning algorithm and it is a gradient descent algorithm. The term back propagation refers to the manner in which the gradient is computed for nonlinear multilayer networks. The flow chart for the back propagation algorithm is given by Benghanem [27]. The activation function for neurons can be

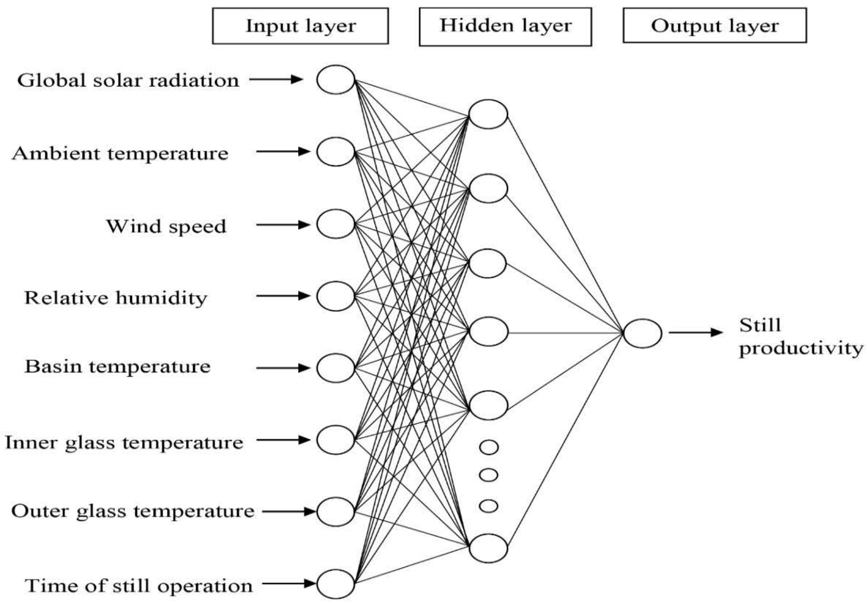


Fig. 3. Functional diagram of the MLP neural network model used in the prediction of still productivity.

linear or nonlinear. Performance of the ANN model is tested by changing the activation functions between input and hidden layers, between hidden and output layer. Activation function suited for present application is suggested.

Tan-sigmoid transfer function (tansig)

$$f(x) = \frac{2}{1+e^{-2x}} - 1 \tag{2}$$

All the datasets were normalized [28] in the range of 0.0–1.0 by using Eq. (3) and then returned to the original values after the simulation by using Eq. (4).

$$X_n = \frac{X_{\text{actual}} - X_{\min}}{X_{\max} - X_{\min}} \tag{3}$$

$$X_{\text{actual}} = X_n \left( X_{\max} - X_{\min} \right) + X_{\min} \tag{4}$$

The best modelling conditions were taken from the references and followed in this study are given in Table 1.

*2.5. Statistical tools considered to assess the performance of the models*

Statistical tools such as the mean percentage error (MPE), mean absolute percentage error (MAPE), relative root mean square error (RRMSE), coefficient of determination ($R^2$), model efficiency (ME) and the OI were used as performance indices to identify the best model. The formulae for MPE, MAPE, RRMSE, $R^2$, ME and OI are presented in Appendix. The model is considered as the best model when MPE, MAPE, and RRMSE, are close to zero and $R^2$, ME and OI values are close to one. These statistical tools are commonly used to evaluate the model performance [22,23,43,44]. Model's performance was described based on the ranges of RRMSE [45] and is given in Table 2.

## 3. Results and discussions

The productivity of the solar still was modelled with MLR and ANN. Total 250 data points were recorded during the experimental period. 190 data points were used in the model development and 60 data points were used to test the developed models. The regression models were developed with the global horizontal solar radiation ($H$), ambient temperature ($T_{amb}$), WS and RH and operational variables, namely basin temperature ($T_{basin}$), inner glass temperature ($T_{inner}$) and outer glass temperature ($T_{outer}$).

The effect of considered parameters on the prediction of solar still productivity was identified with the help of statistical tools and is shown in Table 3.

Table 1
Test conditions followed in this study

| Network type | Multilayer feed forward network [29–34] |
|---|---|
| Training function | TRAINLM [34–38] |
| Adaptive learning function | LEARNGDM |
| Performance function | MSE |
| Number of inputs | 8 |
| Number of outputs | 1 |
| Number of hidden layers | 1 |
| Number of hidden neurons | 15 neurons [22,23,39–42] |
| Transfer function | Tan sigmoid |

Table 2
Ranges of RRMSE to analyse the ANN model's performance

| Range of RRMSE | Performance |
|---|---|
| <10% | Excellent |
| 10% < RRMSE < 20% | Good |
| 20% < RRMSE < 30% | Fair |
| >30% | Poor |

*3.1. Effect of environmental parameters on the solar still productivity*

Effect of environmental variables on prediction of solar still productivity was derived with the help of a regression analysis. Linear regression models developed with the global horizontal solar radiation ($H$), ambient temperature ($T_{amb}$), WS and RH are given below (Eqs. (5)–(8)) and the results were compared with the literature. The maximum and minimum values observed during the experimentation for $H$, $T_{amb}$, WS and RH were 66.57 and 1,073.91 W/m$^2$, 28.14°C and 44.17°C, 2.70 and 12.00 m/s, 37.00% and 87.00%, respectively.

*3.1.1. Solar radiation*

The solar radiation absorbed by the basin material to heat the water mass, which was further evaporated into water vapour and condensed on the glass cover as a distilled water. Okeke et al. [46] concluded that the productivity of the still was directly proportional to the solar radiation. Kamal [47] demonstrated that the still productivity is very much dependent on the solar radiation. The following model was obtained in this work with a lower correlation coefficient indicating that either nonlinear models could be

Table 3
Performance of regression models for new experimental datasets

| MLR model | MPE | MAPE | RRMSE | ME | OI | $R^2$ |
|---|---|---|---|---|---|---|
| $H$ | 56.113 | 87.959 | 39.512 | 0.512 | 0.645 | 0.4560 |
| $T_{amb}$ | 14.496 | 33.654 | 25.761 | 0.792 | 0.823 | 0.7490 |
| $T_{basin}$ | −2.850 | 29.326 | 23.366 | 0.829 | 0.849 | 0.8329 |
| $T_{inner}$ | −4.444 | 21.063 | 14.696 | 0.932 | 0.924 | 0.9193 |
| $T_{outer}$ | −2.729 | 20.892 | 14.418 | 0.935 | 0.926 | 0.9195 |
| WS | 76.535 | 104.589 | 53.838 | 0.095 | 0.396 | 0.1460 |
| RH | 5.190 | 42.390 | 38.840 | 0.529 | 0.655 | 0.5384 |
| Time | 68.118 | 99.703 | 53.286 | 0.113 | 0.406 | 0.1584 |
| **MLR-1** | **−8.489** | **19.542** | **13.935** | **0.939** | **0.930** | **0.9334** |
| MLR-2 | −12.660 | 24.026 | 14.413 | 0.935 | 0.927 | 0.9325 |

The bold value signifies the better statistical values. MLR-1 gives superior performance than other models.

more accurate or more number of additional parameters need to be included in the model for better prediction.

$$Y = 0.292996 + 14.27704 \times H \quad : R^2 = 0.4560 \tag{5}$$

### 3.1.2. Ambient temperature

Researchers all around the world investigated the effect of variation in ambient temperatures on the productivity of solar still, using theoretical model proposed by Malik et al. [48]. The increase in the productivity was 2%–3% with an increase in the ambient temperature of 5°C. Hinai et al. [49] reported an increase in the productivity of solar still by 8.2% with an increase in the ambient temperature of 10°C. The following expression was obtained in this work relating the $T_{amb}$ with yield. The $R^2$ is better than that obtained for $H$, indicating a stronger effect of the sink temperature on the condensate.

$$Y = -765.748 + 25.45717 \times T_{amb} \quad : R^2 = 0.749 \tag{6}$$

### 3.1.3. Wind speed

The rate of heat transfer by convection due to the wind, depends on the temperature difference between the glass outer surface temperature and the ambient temperature. Cooper and Rajvanshi [50,51] concluded that the increase in the WS increases the still productivity. A.A. El-Sebaii [52] concluded that for a single effect passive type basin stills there exist a critical mass (depth of water in the basin) above which the still productivity increases with increase in the wind speed until a typical value ($WS_t$). If the quantity of basin water is less than the critical mass, the still productivity decreases with increase in WS until $WS_t$, also beyond $WS_t$ still productivity becomes less dependent on WS. The results of this work also indicate that the effect of WS is negligible on the yield compared with the effect of $T_{amb}$ and $H$.

$$Y = 17.23732 + 27.25078 \times WS \quad : R^2 = 0.146 \tag{7}$$

## 3.2. Effect of operational parameters on solar still productivity

The productivity of solar still is more dependent on basin temperature ($T_{basin}$), inner glass temperature ($T_{inner}$), outer glass temperature ($T_{outer}$) and less dependent on the time of still operation ($t$) (Table 3). The evaporative heat transfer from the basin water to the glass is directly proportional to the difference between the partial pressure at $T_{basin}$ and $T_{inner}$. Evaporation rate of solar still depends upon the basin water, glass cover and ambient temperature difference. The temperature difference between basin and glass cover is the driving force for the evaporation. Greater is this difference, more is the evaporation of water from the basin. The higher temperature difference between basin and glass could be achieved either by increasing the basin temperature or by decreasing the glass cover temperature. To increase the still productivity, condensation rate should be increased. The condensation rate is dependent on the reduction of inner glass cover temperature. Suneesh et al. [7] reduced the inner glass temperature by intermittent supply of cooling water over the cover.

Effect of operational parameters on prediction of solar still productivity was derived with the help of a regression analysis. Regression models developed with $T_{basin}$, $T_{inner}$, $T_{outer}$ and $t$ are given by Eqs. (8)–(11). The maximum and minimum values observed during the experimentation for $T_{basin}$, $T_{inner}$, $T_{outer}$ and $t$ were 26.43°C and 79.91°C, 32.17°C and 77.75°C, 32.18°C and 77.60°C, 8.00 and 18.00 h, respectively.

Out of all the operational parameters inner and outer glass temperatures have given the highest value of correlation with an $R^2$ value of 0.9193 and 0.9195, respectively. Time of operation has shown the poor correlation with an $R^2$ value of 0.1584.

$$Y = -211.754 + 6.67122 \times T_{basin} \quad : R^2 = 0.8329 \tag{8}$$

$$Y = -321.038 + 8.646793 \times T_{inner} \quad : R^2 = 0.9193 \tag{9}$$

$$Y = -326.608 + 8.806072 \times T_{outer} \quad : R^2 = 0.9195 \tag{10}$$

$$Y = 2.64728 + 15.1882 \times t \quad : R^2 = 0.1584 \tag{11}$$

## 3.3. MLR model

MLR model was developed by considering all the above-mentioned variables to derive the effect of all parameters on prediction of solar still productivity and is given by Eq. (12) and named as MLR-1. MLR-1 has shown an $R^2$ value of 0.93345, which indicates strong relation between selected input variables and output variable.

$$Y = -138.968 - 2.92298 \times t + 5.331446 \times T_{basin} - 14.1145 \times T_{inner} + 21.55639 \times T_{outer} - 10.3788 T_{amb} - 0.0605 \times H + 0.974721 \times WS + 0.618593 \times RH \tag{12}$$

It was observed that the WS, RH and time of operation of solar still have shown the least correlation in the prediction of productivity and other MLR model (MLR-2) was developed by neglecting these parameters and is given by Eq. (13).

MLR-2 gives the relationship between global solar radiation ($H$), all temperature parameters (All $T$'s: $T_{amb}$, $T_{basin,}$ $T_{inner}$, and $T_{outer}$) and solar still productivity with an $R^2$ value of 0.9325 which is equivalent to MLR-1 model.

$$Y = -65.6997 + 3.805568 \times T_{basin} - 15.8259 \times T_{inner} + 24.83606 \times T_{outer} - 12.2704 \times T_{amb} - 0.05888 \times H \tag{13}$$

The developed models (Eqs. (5)–(13)) were tested with the new experimental datasets to assess the performance of regression models. The performance of regression models are shown in Table 3. The solar still output calculated using each model (Eqs. (5)–(13)) was compared with the measured still output during the experimental period and is shown in Fig. 4. It could be observed that the predicted output trend lines of the MLR models followed the actual still output trend line.

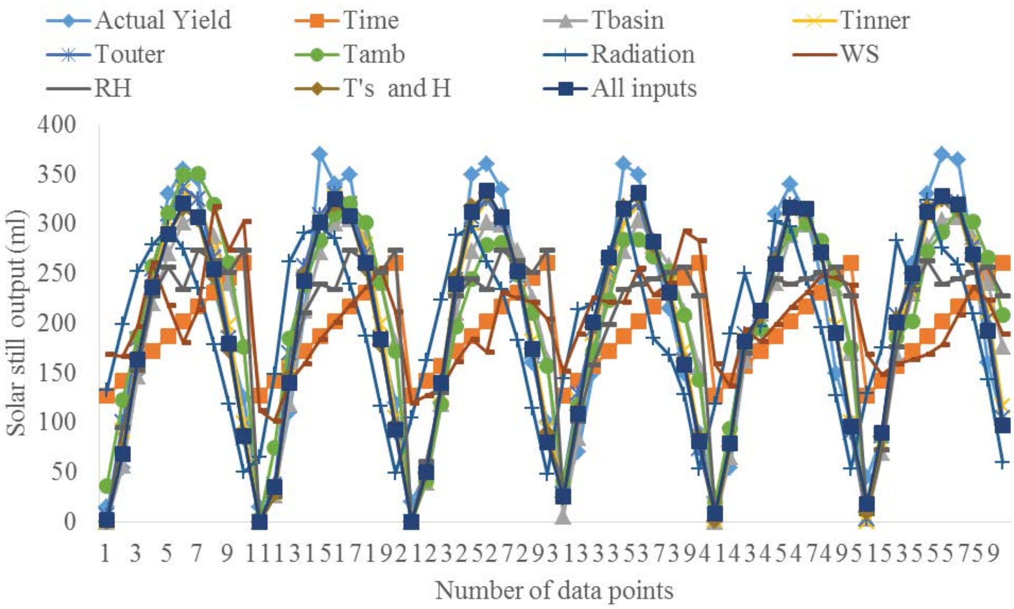


Fig. 4. Actual and predicted still output with regression models.

The results obtained by MLR-1 and MLR-2 were similar compared with the linear regression models with $T_{inner}$ or $T_{outer}$ as the input parameters and indicating strong effect of these variables in prediction of solar still productivity. The regression model developed with WS has shown poor values of performance indices and it could be neglected. It could be observed from Table 3 that the ambient temperature also plays a significant role in the prediction since the ME was 80%. Even though regression models are very basic models, predicted solar still productivity with good accuracy, which reduces the computational time and efforts. Also, eliminates the need of development of complex mathematical equations.

### 3.4. ANN model

In regression analysis, MLR-1 and MLR-2 have shown an excellent prediction of the still productivity with new experimental datasets and the data used for these models were considered for ANN modelling. Test conditions during ANN modelling are shown in Table 1.

A total of eight inputs (all inputs at a time) were used in ANN training and named as ANN-1 and target was still productivity. A total of five inputs (global horizontal solar radiation ($H$), ambient temperature ($T_{amb}$), basin temperature ($T_{basin}$), inner glass temperature ($T_{inner}$) and outer glass temperature ($T_{outer}$)) were used in ANN training and named as ANN-2. These trained ANN models were used in the prediction of still productivity with new experimental datasets (60 new experimental datasets) and results are shown in Table 4. The best values of the performance indices was produced with ANN-1 which considered tan sigmoid transfer function for inner layer to hidden layer and hidden layer to output layer. ANN-2 has also produced the similar performance to that of ANN-1 except the MAPE value which was higher than the MAPE value of ANN-2.

ANN-1 (all inputs) and ANN-2 (all $T$'s and $H$) had produced an excellent prediction of the results and efficiencies of the models were about 96%. The test conditions in Table 1 produced an excellent prediction models and it could be suggested for modelling the solar still productivity.

### 3.5. Comparison between MLR and ANN models

ANN-1 model was developed with the same inputs as that of MLR-1 and ANN-2 model was developed with the same inputs as that of MLR-2. It could be possible to compare ANN-1 with MLR-1 and ANN-2 with MLR-2.

Table 4
Performance of the developed ANN models for new experimental datasets

| ANN model | Inputs to the ANN | MPE (%) | MAPE (%) | RRMSE (%) | ME | OI | Transfer function input layer to hidden layer | Transfer function hidden layer to output layer |
|---|---|---|---|---|---|---|---|---|
| ANN-1 | $H$, $T_{amb}$, WS, RH, $T_{basin}$, $T_{inner}$, $T_{outer}$, $t$ | −3.991 | 14.168 | 11.825 | 0.963 | 0.950 | Tan sigmoid | Tan sigmoid |
| ANN-2 | $H$, $T_{amb}$, $T_{basin}$, $T_{inner}$, $T_{outer}$ | −8.238 | 13.845 | 11.895 | 0.962 | 0.950 | Tan sigmoid | Tan sigmoid |

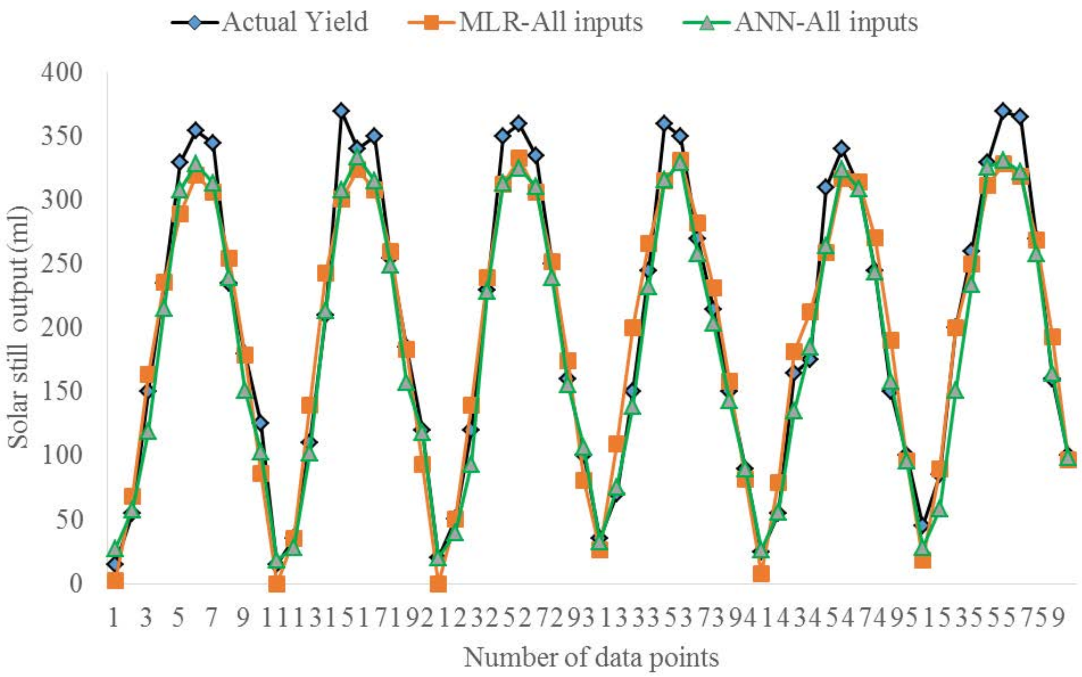


Fig. 5. Comparison of MLR-1 and ANN-1 models predicted still output values with actual still output.

While comparing ANN-1 with MLR-1, 27.53% improvement in MAPE values, 15.14% improvement in RRMSE, 2.44% improvement in ME and 2.15% improvement in OI were observed and shows superior performance of ANN-1 than MLR-1.

While comparing ANN-2 with MLR-2, 42.44% improvement in MAPE values, 17.48% improvement in RRMSE, 2.88% improvement in ME and 2.15% improvement in OI were observed and shows superior performance of ANN-2 than MLR-2. The predicted output of MLR-1 and ANN-1 models were compared with actual still output values and is shown in Fig. 5.

## 4. Conclusion

MLR and ANN models were developed to predict the yield of solar still using weather and operational data. The linear regression models with operational parameters such as $T_{\text{inner}}$ and $T_{\text{outer}}$ have given an excellent estimation out of the linear models with the ME values more than 90%. The operational parameters have shown higher impact than the environmental parameters on the yield, indicating that the condenser temperature has got the highest correlation with respect to the yield. In other words the overall productivity of the still could be made better by altering the condenser temperature.

It could also be observed that out of the environmental parameters, the ambient temperature played the most significant in role in the estimation of still yield, indicating the importance of the sink temperature on the yield. The developed MLR-1 and MLR-2 have shown an excellent performance in the estimation of still yield. Two ANN models were developed with the selected input variables by considering tan sigmoid as the transfer function. ANN-1 and ANN-2 models have almost produced similar performance and revealing the insignificant effect of WS and RH in the model's performance and hence they could be neglected in modelling the estimation of solar still output development. ANN-1 and ANN-2 models outperformed the developed MLR-1 and MLR-2 models.

## Appendix

$$\text{MPE} = \frac{1}{p}\sum_{i=0}^{p}\left(\frac{H_{i,e}-H_{i,m}}{H_{i,m}}\right)\times 100$$

$$\text{MAPE} = \frac{1}{p}\sum_{i=0}^{p}\left|\frac{H_{i,e}-H_{i,m}}{H_{i,m}}\right|\times 100$$

$$\text{RRMSE} = \frac{\sqrt{\left(\frac{1}{p}\sum_{i=1}^{p}\left(H_{i,e}-H_{i,m}\right)^2\right)}}{\frac{1}{p}\sum_{i=1}^{n}H_{i,m}}\times 100$$

$$\text{OI} = \frac{1}{2}\left(1-\left(\frac{\text{RMSE}}{x_{\max}-x_{\min}}\right)+\text{ME}\right)$$

$$\text{ME} = 1-\frac{\sum_{i=1}^{n}\left(x_{a,i}-x_{f,i}\right)^2}{\sum_{i=1}^{n}\left(x_{a,i}-\overline{x_{a,i}}\right)^2}$$

## Symbols

*Abbreviations*

| | | |
|---|---|---|
| AI | — | Artificial intelligence |
| ANN | — | Artificial neural network |
| EC | — | Electrical conductivity, μS/cm |
| GHI | — | Global horizontal radiation, W/m$^2$ |
| $H$ | — | Global horizontal solar radiation, W/m$^2$ |
| LM | — | Levenberg–Marquardt |
| MAPE | — | Mean absolute percentage error |
| ME | — | Model efficiency |
| MLP | — | Multilayer perception |
| MLRs | — | Multiple linear regressions |
| MPE | — | Mean percentage error |
| MSE | — | Mean square error |
| MVR | — | Multivariate regression |
| NARX | — | Nonlinear autoregressive exogenous networks |
| OI | — | Overall index of model performance |
| $R^2$ | — | Coefficient of determination |
| RH | — | Relative humidity, % |
| RRMSE | — | Relative root mean square error |
| $T$ | — | Temperature, °C |
| $t$ | — | Time of still operation, h |
| TDS | — | Total dissolved solids, mg/L |
| WS | — | Wind speed, m/s |
| $Y$ | — | Yield of solar still, mL |

*Subscripts*

| | | |
|---|---|---|
| inner | — | Inner glass surface |
| amb | — | Ambient |
| outer | — | Outer glass surface |
| $t$ | — | Typical |

*Greek letters*

| | | |
|---|---|---|
| β | — | Condensing cover tilt angle, degree |

## References


[1] S. Bhawan, R.K. Puram, $CO_2$ Baseline Database for the Indian Power Sector User Guide Government of India Ministry of Power Central Electricity Authority, 2014, Available at: http://cea.nic.in/reports/others/thermal/tpece/cdm_co2/user_guide_ver10.pdf.

[2] H. Sharon, K.S. Reddy, Performance investigation and enviro-economic analysis of active vertical solar distillation units, Energy, 84 (2015) 794–807.

[3] V.K. Dwivedi, G.N. Tiwari, Thermal modeling and carbon credit earned of a double slope passive solar still, Desal. Wat. Treat., 13 (2012) 400–410.

[4] T. Rajaseenivasan, K. Srithar, Performance investigation on solar still with circular and square fins in basin with $CO_2$ mitigation and economic analysis, Desalination, 380 (2016) 66–74.

[5] India Solar Resource Maps, Global Horizontal Irradiance-Annual Average, Available at: https://www.nrel.gov/international/images/india_ghi_ annual.jpg (last accessed on 26th June 2018).

[6] M.K. Phadatare, S.K. Verma, Influence of water depth on internal heat and mass transfer in a plastic solar still, Desalination, 217 (2007) 267–275.

[7] P.U. Suneesh, R. Jayaprakash, T. Arunkumar, D. Denkenberger, Effect of air flow on "V" type solar still with cotton gauze cooling, Desalination, 337 (2014) 1–5.

[8] Y. Taamneh, M.M. Taamneh, Performance of pyramid-shaped solar still: experimental study, Desalination, 291 (2012) 65–68.

[9] M.H. Sellami, R. Touahir, S. Guemari, K. Loudiyi, Use of Portland cement as heat storage medium in solar desalination, Desalination, 398 (2016) 180–188.

[10] P.K. Srivastava, S.K. Agrawal, Experimental and theoretical analysis of single sloped basin type solar still consisting of multiple low thermal inertia floating porous absorbers, Desalination, 311 (2013) 198–205.

[11] S. Abdallah, M.M. Abu-Khader, O. Badran, Effect of various absorbing materials on the thermal performance of solar stills, Desalination, 242 (2009) 128–137.

[12] K.K. Murugavel, S. Sivakumar, J.R. Ahamed, K.K.S.K. Chockalingam, K. Srithar, Single basin double slope solar still with minimum basin depth and energy storing materials, Appl. Energy, 87 (2010) 514–523.

[13] H.S. Deshmukh, S.B. Thombre, Solar distillation with single basin solar still using sensible heat storage materials, Desalination, 410 (2017) 91–98.

[14] F.F. Tabrizi, A.Z. Sharak, Experimental study of an integrated basin solar still with a sandy heat reservoir, Desalination, 253 (2010) 195–199.

[15] T. Arunkumar, D. Denkenberger, A. Ahsan, R. Jayaprakash, The augmentation of distillate yield by using concentrator coupled solar still with phase change material, Desalination, 314 (2013) 189–192.

[16] A.E. Kabeel, M. Abdelgaied, Improving the performance of solar still by using PCM as a thermal storage medium under Egyptian conditions, Desalination, 383 (2016) 22–28.

[17] T. Arunkumar, R. Jayaprakash, D. Denkenberger, A. Ahsan, M.S. Okundamiya, S. Kumar, H. Tanaka, H.Ş. Aybar, An experimental study on a hemispherical solar still, Desalination, 286 (2012) 342–348.

[18] H.E. Gad, S. Shams El-Din, A.A. Hussien, K. Ramzy, Thermal analysis of a conical solar still performance: an experimental study, Sol. Energy, 122 (2015) 900–909.

[19] R. Sathyamurthy, H.J. Kennady, P.K. Nagarajan, A. Ahsan, Factors affecting the performance of triangular pyramid solar still, Desalination, 344 (2014) 383–390.

[20] A.E. Kabeel, Performance of solar still with a concave wick evaporation surface, Energy, 34 (2009) 1504–1509.

[21] M.R. Karimi Estahbanati, A. Ahsan, M. Feilizadeh, K. Jafarpur, S.S. Ashrafmansouri, M. Feilizadeh, Theoretical and experimental investigation on internal reflectors in a single-slope solar still, Appl. Energy, 165 (2016) 537–547.

[22] A.F. Mashaly, A.A. Alazba, A.M. Al-awaadh, M.A. Mattar, Predictive model for assessing and optimizing solar still performance using artificial neural network under hyper arid environment, Sol. Energy, 118 (2015) 41–58.

[23] A.F. Mashaly, A.A. Alazba, MLP and MLR models for instantaneous thermal efficiency prediction of solar still under hyper-arid environment, Comput. Electron. Agric., 122 (2016) 146–155.

[24] M.A. Hamdan, R.A.H. Khalil, E.A.M. Abdelhafez, Comparison of Neural network models in the estimation of the performance of solar still under Jordanian climate, J. Clean Energy Technol., 1 (2013) 238–242.

[25] N.I. Santos, A.M. Said, D.E. James, N.H. Venkatesh, Modeling solar still production using local weather data and artificial neural networks, Renewable Energy, 40 (2012) 71–79.

[26] A.F. Mashaly, A.A. Alazba, Comparative investigation of artificial neural network learning algorithms for modeling solar still production, J. Water Reuse Desal., (2015) 480–493.

[27] M. Benghanem, A. Mellit, S.N. Alamri, ANN-based modelling and estimation of daily global solar radiation data: a case study, Energy Convers. Manage., 50 (2009) 1644–1655.

[28] A. Rahimikhoob, Estimating global solar radiation using artificial neural network and air temperature data in a semi-arid environment, Renewable Energy, 35 (2010) 2131–2135.

[29] K.S. Reddy, M. Ranjan, Solar resource estimation using artificial neural networks and comparison with other correlation models, Energy Convers. Manage., 44 (2003) 2519–2530.

[30] M.N.Q. Macedo, J.J.M. Galo, L.A.L. de Almeida, A.C. de C. Lima, Demand side management using artificial neural networks in a smart grid environment, Renewable Sustainable Energy Rev., 41 (2015) 128–133.

[31] J. Mubiru, E.J.K.B. Banda, Estimation of monthly average daily global solar irradiation using artificial neural networks, Sol. Energy, 82 (2008) 181–187.
[32] J. Wasilewski, D. Baczynski, Short-term electric energy production forecasting at wind power plants in pareto-optimality context, Renewable Sustainable Energy Rev., 69 (2017) 177–187.
[33] T. Khatib, A. Mohamed, K. Sopian, M. Mahmoud, Solar energy prediction for Malaysia using artificial neural networks, Int. J. Photoenergy, 2012 (2012) 1–16.
[34] R. Kumar, R.K. Aggarwal, J.D. Sharma, Comparison of regression and artificial neural network models for estimation of global solar radiations, Renewable Sustainable Energy Rev., 52 (2015) 1294–1299.
[35] H. Chitsaz, H. Shaker, H. Zareipour, D. Wood, N. Amjady, Short-term electricity load forecasting of buildings in microgrids, Energy Build., 99 (2015) 50–60.
[36] A.K. Tossa, Y.M. Soro, Y. Azoumah, D. Yamegueu, A new approach to estimate the performance and energy productivity of photovoltaic modules in real operating conditions, Sol. Energy, 110 (2014) 543–560.
[37] A.K. Yadav, S. Chandel, Artificial neural network based prediction of solar radiation for Indian stations, Int. J. Comput. Appl., 50 (2012) 1–4.
[38] L. Mba, P. Meukam, A. Kemajou, Application of artificial neural network for predicting hourly indoor air temperature and relative humidity in modern building in humid region, Energy Build., 121 (2016) 32–42.
[39] M. Ozgoren, M. Bilgili, B. Sahin, Estimation of global solar radiation using ANN over Turkey, Expert Syst. Appl., 39 (2012) 5043–5051.
[40] A.K. Yadav, H. Malik, S.S. Chandel, Selection of most relevant input parameters using WEKA for artificial neural network based solar radiation prediction models, Renewable Sustainable Energy Rev., 31 (2014) 509–519.
[41] A.K. Yadav, S.S. Chandel, Solar radiation prediction using Artificial Neural Network techniques: a review, Renewable Sustainable Energy Rev., 33 (2014) 772–781.
[42] A.F. Mashaly, A.A. Alazba, Neural network approach for predicting solar still production using agricultural drainage as a feedwater source, Desal. Wat. Treat., 57 (2016) 28646–28660.
[43] A. Teke, H.B. Yıldırım, Ö. Çelik, Evaluation and performance comparison of different models for the estimation of solar radiation, Renewable Sustainable Energy Rev., 50 (2015) 1097–1107.
[44] E. Paulescu, R. Blaga, Regression models for hourly diffuse solar radiation, Sol. Energy, 125 (2016) 111–124.
[45] M.F. Li, X.P. Tang, W. Wu, H. Bin Liu, General models for estimating daily global solar radiation for different solar radiation zones in mainland China, Energy Convers. Manage., 70 (2013) 139–148.
[46] E. Okeke, S.U. Egarievwe, A.E. Anmalu, Effects of coal and charcoal on solar-still performance, Energy, 15 (1990) 1071–1073.
[47] W.A. Kamal, A theoretical and experimental study of the basin-type solar still under the Arabian gulf climatic conditions, Solar Wind Technol., 5 (1988) 147–157.
[48] M.A.S. Malik, G.N. Tiwari, A. Kumar, M.S. Sodha, Solar Distillation, Pergamon Press, Oxford, 1982.
[49] S.M. Al-Alawi, H.A. Al-Hinai, An ANN-based approach for predicting global radiation in locations with no direct measurement instrumentation, Renewable Energy, 14 (1998) 199–204.
[50] P.I. Cooper, Digital simulation of transient solar still processes, Sol. Energy, 12 (1969) 313–331.
[51] A.K. Rajvanshi, Effect of various dyes on solar distillation, Sol. Energy, 27 (1981) 51–65.
[52] A.A. El-Sebaii, Effect of wind speed on active and passive solar stills, Energy Convers. Manage., 45 (2004) 1187–1204.